Value of broadband seismic for interpretation, reservoir characterization and quantitative interpretation workflows

Cyrille Reiser,[1*] Tim Bird,[1] Folke Engelmark,[1] Euan Anderson[1] and Yermek Balabekov[1] present a series of case studies to illustrate the performance of broadband seismic dual-sensor streamer acquisition and its positive impact across a range of E&P asset development phases from exploration to appraisal and field development/optimization.

To be successful in the more challenging E&P environments being explored and developed today petroleum geoscientists need to detect and properly image very complex reservoirs and be able to resolve the fine detail of thinner reservoir units and remaining hydrocarbon columns. To meet these challenges geoscientists would like seismic data that fulfil a demanding set of expectations: to identify and delineate prospects based on amplitude and/ or attributes response, both from post-stack and pre-stack domains; to describe the internal structure of the reservoir; to depth convert the seismic; and to characterize or quantify key reservoir properties such as porosity and increase the probability of successfully discriminating lithology-fluid facies. All these goals need to be achieved in 3D using all the dimensions of the seismic data (pre-stack 3D and 4D).

The holy grail of reservoir geoscientists seeking to optimize the locations of costly wells is to be able to discern the physical properties of rock formations in the earth before they drill. Until now seismic images have fallen short of delivering on this goal. Most of the seismic interpretation and reservoir characterization work performed to date has had to rely on using relatively 'narrow' bandwidth seismic datasets, or with seismic data that has a spectrum preferentially skewed towards the low side or the high side of the frequency range, but in all cases without the full frequency spectrum that would enable the 'full' picture to be seen and characterized.

A severe limitation on seismic imaging has always been the ghost reflections from the sea surface that occur both at the source and the receiver side. These undesired reflections significantly degrade the seismic image and compromise the interpretation and quantitative analysis of seismic data by creating some non-geological events. In 2007, Petroleum Geo-Services introduced the dual-sensor streamer with two sensors (pressure and vertical particle velocity) co-located in the streamer (Carlson et al., 2007). This streamer configuration allows the receiver ghost to be removed by separating

the up- and down-going wavefields and also facilitates towing the streamer deeper (>15m) increasing the seismic acquisition weather window. This acquisition system has enabled an extension of seismic bandwidth at both the low and high ends of the frequency spectrum and has been used extensively in 2D and 3D mode over many regions and basins across the world.

The broader bandwidth enabled by the removal of the receiver ghost (Söllner, 2007) has crucial advantages at both ends of the frequency spectrum and more recently, this de-ghosting has also been developed for the source side. By having a time and depth distributed source the new design has allowed the removal of the source ghost (Parkes et al., 2011 and Parkes and Hegna, 2011). Eliminating both the source and receiver ghosts dramatically increases the seismic bandwidth (Reiser et al., 2012).

The potential benefits provided by broadband seismic can be demonstrated by means of simple modelling.

Figure 1 show a suite of wavelets where the bandwidth is extended by one octave at both ends for each consecutive wavelet. The first observation is that the dominant bandwidth is almost identical to the upper limit of the pass-band. The second key observation is that the side-peak/lobe amplitude ratio is increasing with increasing bandwidth in octaves. This effect is independent of which end the frequency spectrum extension is achieved. The higher concentration of seismic energy in the main peak compared to the side lobes in broadband seismic data is an important aspect of seismic interpretability as it reduces the likelihood of erroneously interpreting the side-lobes as real responses to impedance boundaries. A sharper wavelet also reduces seismic tuning effects.

The 2D wedge model shown in Figure 2 provides additional insight into the benefits resulting from bandwidth extension at both the low and high ends of the spectrum.

A simple 2D wedge model was designed with three layers of sand tapering from 30 ms thickness and pinching out

[1] Petroleum Geo-Services.

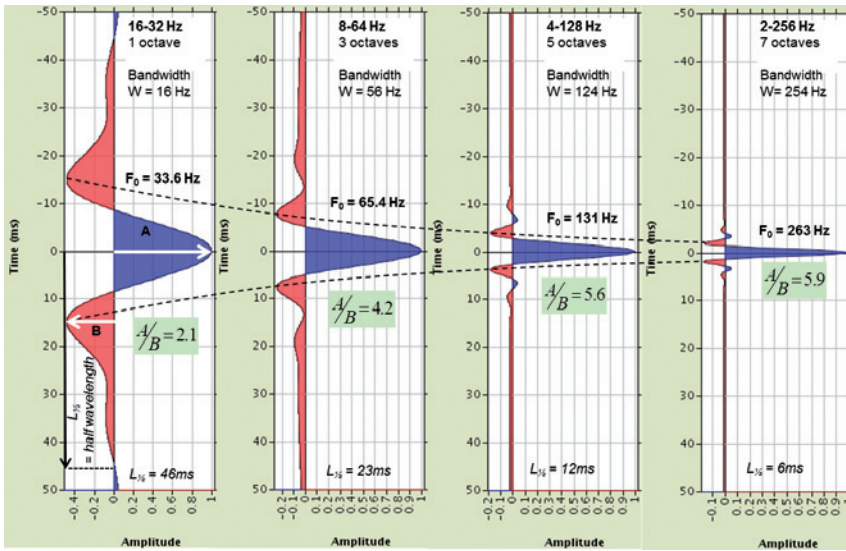[*] Corresponding author, E-mail: cyrille.reiser@pgs.com

Figure 1 Wavelet modelling at different band-widths (to the left) where the frequency extension is incremented by one octave at both sides for each wavelet, resulting in wavelets of 1, 3, 5, and 7 octaves. Dominant frequency (F0) is annotated in bold. The green boxes show the peak/ sidelobe amplitude ratio which increases with higher bandwidth in octaves. Annotated at the bottom is half of the wavelength for each wavelet.
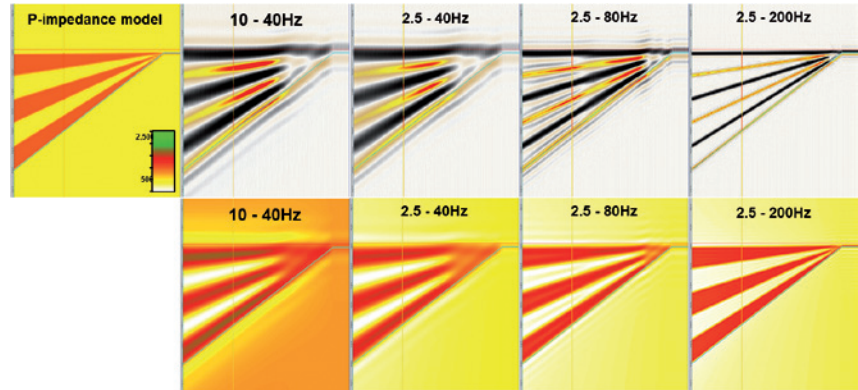

Figure 2 Wedge model showing seismic responses for wavelets of different bandwidth. The four top right images illustrate the seismic responses for the various wavelets and the four bottom images illustrate the impedance inversions based on the modelled seismic. The colour palette for the impedance sections are identical. Each wedge tapers from 30 ms at the edge.

to 0 ms (upper left image). This model was then convolved with wavelets composed of a range of different bandwidths from 20–40 Hz (representing conventional bandwith) up to 2.5–200 Hz to produce the corresponding synthetic seismic responses (upper reflectivity images). The synthetic seismic responses were then band-limited and 'inverted' into relative impedance responses (lower responses). This simple modelling illustrates an increasingly clear delineation of the top and base of each individual layer as a result of the contribution of the increasing low and high frequencies.

The model illustrates that broadband bandwidth extension (2.5–200 Hz) results in an impedance response close to the original acoustic impedance model: thin layers are resolved in the high frequency part of the spectra, and the *absolute* values of impedance are accurately recovered the contribution of the low frequency part (with the yellow colour of the background closely matching the initial model).

The important contribution of the low frequency component is clearly highlighted by comparing the difference in model response between 20–40 Hz and 2.5-40 Hz scenarios.

Thus, the high frequencies are crucial for vertical resolution while the low frequencies are important for depth penetration and low frequency model building. The extension of low frequencies will reduce the need for complex background models to convert relative properties to absolute properties for parameters such as P-impedance and Vp/Vs (Reiser, 2011). The combined effect of extending both the high frequencies and the low frequencies will be to provide a relative inversion result that is closer to the absolute elastic properties, as fewer Hertz will be missing on the low side of the spectra.

The high end of the bandwidth extension can also be seen in Figure 3, which illustrates the extended bandwidth at the wavelet level from a real broadband seismic dataset. The wavelets shown were extracted at the water bottom and demonstrate that with a conventional acquisition (left hand-side) the peak of the wavelet is relatively broad and a significant amount of side lobe energy is present (as a result of source and streamer ghosts), whereas the wavelet from the broadband seismic (receiver *and* source ghosts removed in this case) shows almost no side lobes and a very narrow peak. Such a sharp wavelet will enable the imaging of very thin layers that previously have not been possible to resolve using conventional limited-bandwidth seismic.

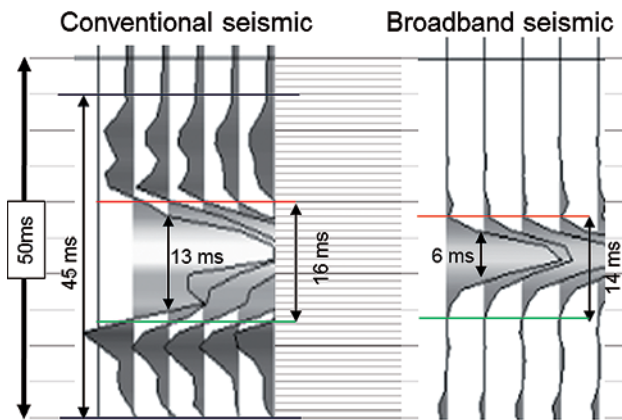# Reservoir Geoscience and Engineering

Figure 3 Extracted wavelets at the water bottom from a conventional acquisition (left hand-side) and broadband ghost- free solution (right hand-side).

Case studies

Having laid the groundwork and the rationale behind broadband seismic, the benefits are now illustrated using various case studies from different geological settings and different stages of maturity in the E&P asset life. The case studies are subdivided into specific benefits such as interpretability and estimation of elastic properties.

Interpretability

In 2011, PGS acquired 2D seismic data over the Møre Marginal High offshore Norway (Figure 4) with a dual-sensor streamer and a time-depth distributed source. The regional geology here is dominated by deep Cretaceous sediments, overlain by Eocene basalt flows and volcanic intrusives as well as recent slump structures (Faerseth et al., 2008). The quality of the seismic image allows the various sequence units to be clearly identified, as well as the geological structure and internal geometry. The seismic quality and bandwidth (2.5 to more than 175 Hz) reveal geological and structural detail that has never been seen before in this region.

With a seismic image so rich in frequencies at both low and high sides, the benefits for interpretation purposes alone are significant allowing the seismic interpreter to evaluate the geology more accurately as less artifact contamination is present in the seismic section. Instead of interpreting a seismic image degraded with side lobes and exhibiting a lack of resolution, this type of seismic image quality reveals the earth response much closer in appearance to a true geological outcrop view.

With such a frequency-rich spectrum broadband seismic allows the interpretation geoscientist to see subsurface geology in unprecedented detail and fidelity, with significantly less degradation by the ghost-related artifacts.

Seismic inversion of this high-resolution broadband de-ghosted data is even more illuminating. The results of pre-stack relative simultaneous inversion of a portion of this line are illustrated in Figure 5. The type of stratigraphic wedge presented in the synthetic model results in Figure 2 can be observed in this real dataset (upper right seismic feature).

Figure 4 Example of a 2D seismic line over the Møre Margin High in Norway to the north of the Faroes Shetland Basin. The line was acquired with a ghost-free acquisition system comprising dual-sensor towed streamer and time and depth distributed source.
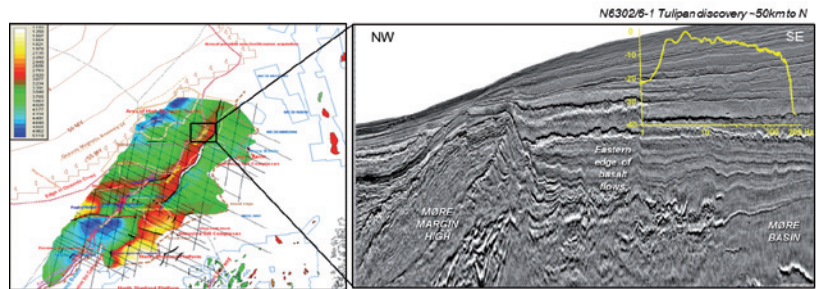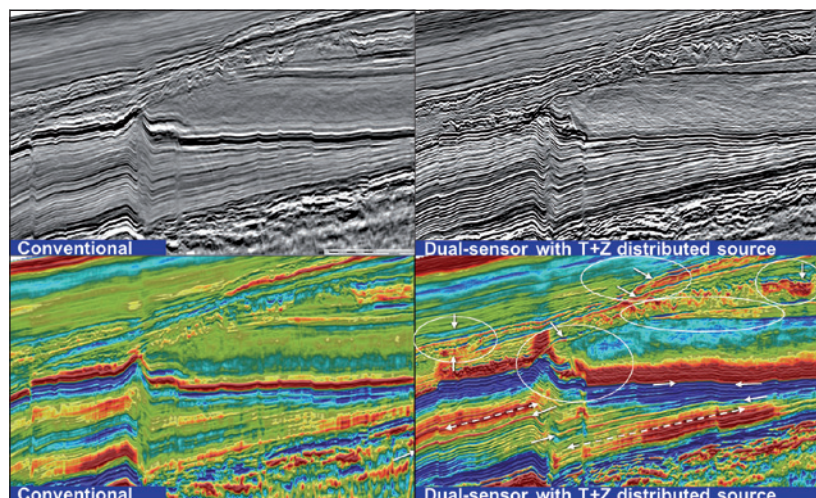

Figure 5 Zoom in on part of the Møre Margin High (Norway) 2D seismic line contrasting the conventional seismic response (left hand side) and the result with a ghost-free acquisition system (dual-sensor towed streamer and time and depth distributed source) on the right hand-side. The lower images show their corresponding relative acoustic impedance responses.

With this real data the geological wedge is faithfully resolved down to a limit of less than 3 m demonstrating again the importance of the extended bandwidth at the high side of the frequency spectrum.

Relative elastic properties derivation

Broadband seismic data are particularly rich on the low side of the frequency spectra, therefore during the seismic inversion process the need to add low frequency data from well information or an a priori model is considerably reduced. This can be demonstrated in practice using the results from a North Sea dataset where recent dual-sensor acquisition and processing was performed over a 3D area in the North Viking Graben in the vicinity of the Heimdal and Frigg fields (Figure 6).

The results of a pre-stack relative seismic inversion workflow conducted on the Heimdal area are presented
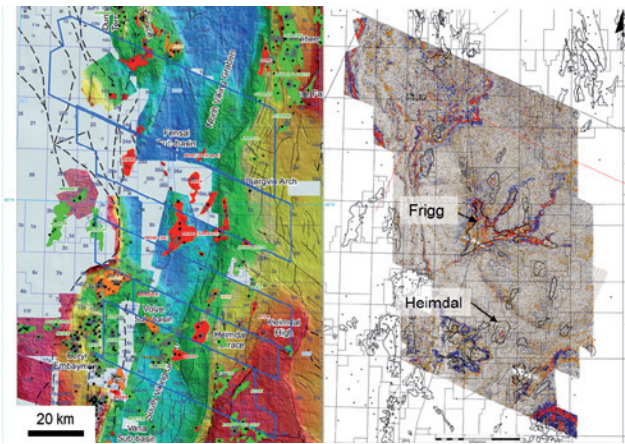

Figure 6 Map and time-slice views of the North Viking Graben seismic used for quantitative interpretation analysis. The Frigg (Eocene age) and the Heimdal (Palaeocene age) fields are both gas reservoirs. Both fields are sandstone reservoirs deposited in a deep marine environment and are now abandoned as depleted. The map on the right hand-side illustrates a time slice through the recently acquired and processed dual-sensor streamer seismic. This represents close to 6000 km2 of pre-stack data.

in Figure 7. The pre-stack relative inversion was initially performed without a low frequency model derived from the combination of the seismic velocity and the well information which is traditionally performed in the industry. Instead, first the seismic velocity information used for the flatness of the PSTM gathers (the RNMO velocity field) has been converted to interval velocity using the Dix equation. Then, this interval velocity was multiplied by an average Tertiary density of 2.35 g.cm^3 to provide an approximate transform of relative acoustic impedance to 'absolute' impedance that produces a low frequency model derived solely from the seismic data. This seismically-derived low frequency model was then added to the relative elastic attributes extracted from the seismic to transform to 'absolute' attributes. Using this workflow an 'absolute' seismic inversion result has been estimated without using wells information as calibration points for the velocity model. Using this approach the resulting 'absolute' impedance volume is derived solely from seismic information. Figure 9 illustrates the result of this 'absolute' acoustic impedance. This is compared at the well location to the same attribute measured from the well log data which has been filtered to seismic bandwidth. The trace of the acoustic impedance from the seismic inversion closely matches the (filtered) acoustic impedance log at the well location.

This analysis demonstrates that, with good processing, the broadband seismic delivered can be used directly to derive elastic attributes that are remarkably close to the calibrated ground truth. This approach works based on the fact that the seismic frequency bandwidth of these data is very rich on the low side, which minimizes the need for extra information to fill the low frequency gap. And even the minimal remaining gap at the ultra-low end can be adequately filled by using the velocity information contained in the broadband seismic (which is also more accurate and more reliable).
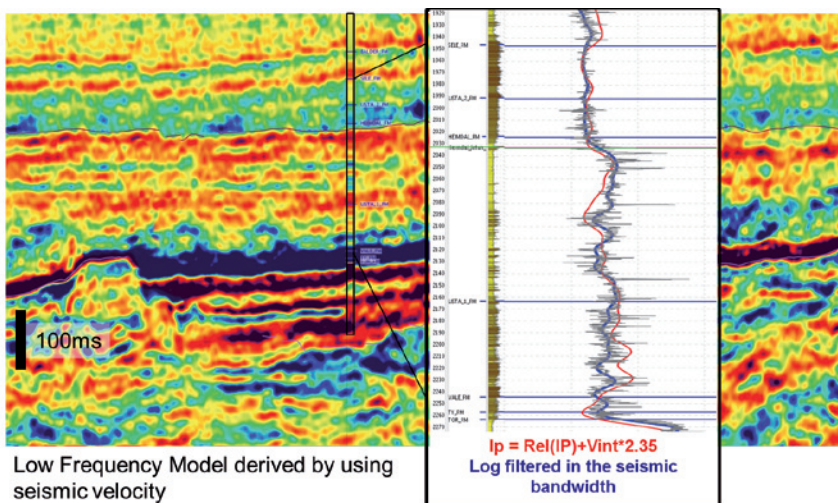

Low Frequency Model derived by using seismic velocity

Ip = Rel(IP)+Vint*2.35
Log filtered in the seismic bandwidth

Figure 7 'Absolute' acoustic impedance result compared with the acoustic impedance from logs at the well. The absolute acoustic impedance has been derived by performing a pre-stack seismic inversion of the dual-sensor towed streamer dataset and by adding an equivalent acoustic impedance model computed from the seismic velocity only. The match at the well location of this entirely seismic driven acoustic impedance is very encouraging.

This example demonstrates the potential to use pre-stack inversion of broadband seismic data to evaluate the acoustic/elastic impedance response away from well control with a relatively high degree of confidence as there is no reliance on any a priori information from sparsely-spaced well data which could bias the inversion analysis. And this approach with broadband data can be expected to yield useful results even when no well information is available in an area.

The next case study from the Browse Basin in Australia illustrates the benefits of using relative inversion derived from broadband seismic, this time focusing on better imaging of the fluid contact.

The seismic line used is located in a known gas province of the North West Shelf of Australia. The stratigraphic sequence comprises Permo-Triassic sediments overlain by Jurassic to Cenozoic syn- and post-rift successions (Longley et al., 2003). In the same acquisition programme 2D seismic data were acquired along this line location with modern conventional streamer configuration and with dual-sensor streamer technology. The results of a relative pre-stack inversion workflow performed on these two datasets are presented in Figures 8 and 9. The workflow used in this case follows the method described by Thompson, 2011. It is equivalent to the extended elastic impedance (EEI) methodology developed by Whitcombe (2002). In this approach, instead of performing the coloured intercept-gradient rotation according to a chi angle matching a well property, the rotation is performed in the angle stacks domain. This has the benefit of working in a statistically independent space, with higher signal-to-noise ratio and the rotation angle can be related directly to rock physics analysis. In this case, the rotation angle is performed in the inverted space (relative pre-stack inversion of the near and far stacks).

In this study the rotation between the angle stacks was performed to maximize the gas response (figure 8), as this is the main hydrocarbon fluid present in this data.
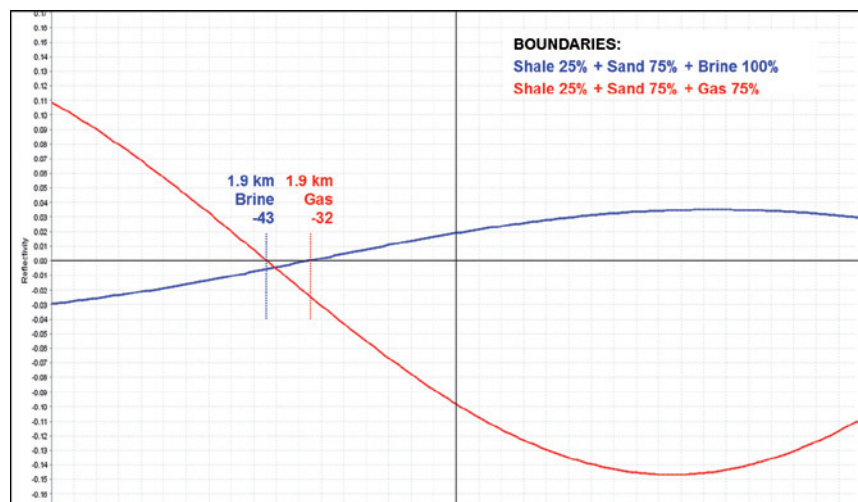
Figure 8 Modelling of reflectivity (relative impedance) response versus AVA rotation angle for two litho-fluid scenario interfaces (shale overlying brine sand is presented in blue and shale overlying gas sands is presented in red). At the top of the reservoir the angle at which the response for brine sands is minimized and the response for the gas sands is maximized is predicted to be -32°.
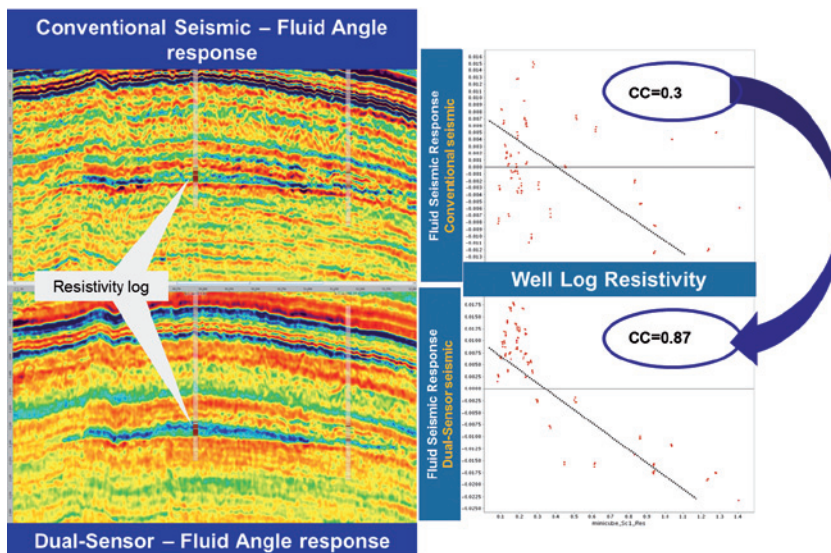
Figure 9 Comparison of inversion results (fluid angle) for conventional streamer and dual-sensor seismic acquisition.

Reservoir Geoscience and Engineering

The fluid angle results for conventional and dual-sensor datasets are shown in Figure 9. Compared to the conventional seismic data (top, figure 9) the AVA rotation section for the dual-sensor streamer seismic data (the bottom, figure 9) shows clearer definition of geological units with improved resolution of the geometry, extend the gas sands interval and a sharper gas-water contact.

For a semi-quantitative assessment of the improvement, the AVA stack rotation response at the optimized fluid angle of -32^0 was extracted along the borehole and compared to the resistivity log. The cross-plots (right hand-side, Figure 9) show a marked improvement of correlation (0.87 as opposed to 0.3), as measured by the correlation coefficient (CC) between the rotated angle stack response using dual-sensor streamer compared to the conventional seismic. This indicates numerically that the broadband seismic data estimates gross fluid volume substantially more accurately than conventional seismic data.

**Improved well placement in 3D**

The next case study example, based on a 3D seismic dataset over the Heimdal field in the North Sea, examines the advantage for quantitative reservoir characterization from the broadband nature of dual-sensor data. In a previous section, it was demonstrated that having a broader seismic frequency bandwidth enables elastic properties to be derived more reliably away from the well control points (or calibration points used for building an a priori low frequency model) because the broader bandwidth at the low end reduces or eliminates the need for a low frequency model biased by well or a priori information.

The objective of this case study was to investigate the impact on elastic properties prediction away from the well control, and the importance of a low frequency model below seismic bandwidth. Two cases were analyzed and compared.

In both cases, the low frequency model was built using well log information and seismic NMO velocity information to fill the gap in frequency spectrum below seismic bandwidth. Pre-stack simultaneous inversion was performed with the same parameters for both datasets. The only difference between the two datasets is the amount of low frequency model information that needed to be 'injected' into the inversion process. The first case represents a typical scenario with conventional seismic bandwidth. With a realistic seismic bandwidth at the reservoir level of 10-30 Hz, the inversion has to rely on a low frequency model up to 10 Hz, based on information from sparse well locations, to fill the frequency gap below seismic bandwidth.

The second case represents dual-sensor streamer broadband seismic data containing an additional octave of low frequencies and which therefore requires a narrower low frequency model only from 0 to 5 Hz (many dual-sensor datasets show useful signal down to as low as 3–4 Hz). This frequency gain of an octave on the low side is equivalent to a gain in the high frequency from 25 Hz to 50 Hz. Several case studies examined show as much as two octaves of gain on the low side of the spectrum.

Figure 12 illustrates the results over the Heimdal field area of the pre-stack inversion using the two seismic versions. In this example, the low frequency model and inversion were performed using the two outer wells as input control points and the results evaluated against the central 'blind' well. The outer two control wells are more than 20 km apart. By looking at the match between the inversion results at the 'blind' well and the actual well values, the match of the pre-stack inversion can be evaluated in section view and in a well tie view (right hand side of Figure 10). It can be seen that the elastic attributes estimated at the blind well are improved with the inversion results from the broadband scenario, relying more on seismic input and using only 0–5Hz of low frequency model, as opposed
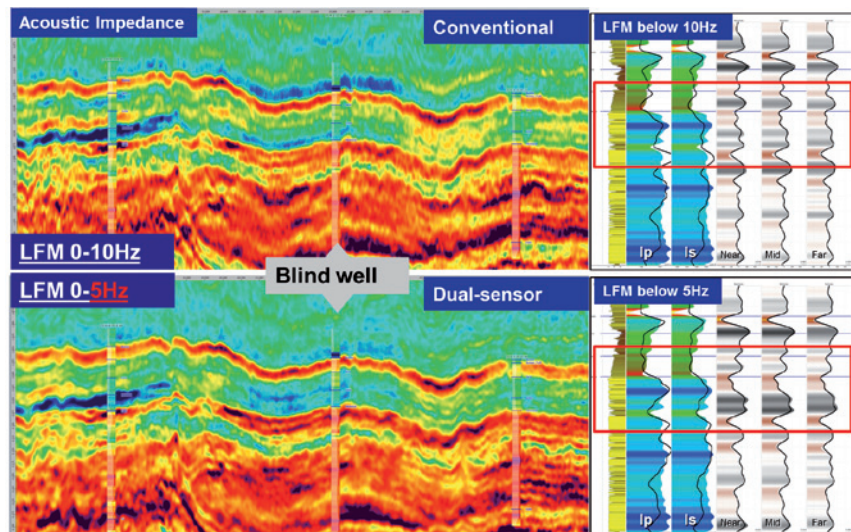
Figure 10 Comparison of two acoustic impedance results based on pre-stack seismic inversion using two different initial low frequency models (LFM), dependent on the bandwidth of the seismic data input. Top figure corresponds to the conventional acquisition results and the bottom corresponds to the dual-sensor streamer inversion results.

to the conventional bandwidth scenario with 0–10Hz of low frequency information derived from well data which shows a poorer match to the blind well in section and log view. The dual-sensor data shows no discernible degradation in vertical resolution of the seismic data or inversion result.

This case study demonstrates that the ability to predict the reservoir properties away from calibration wells is improved due to the extended low frequency bandwidth offered by the dual-sensor streamer. This improved match to ground truth gives increased confidence in the results of this type of pre-stack inversion of broadband seismic data away from well control. In this case broadband solutions provide significant added value for well placement. In such cases there is a demonstrable value-of-information benefit from dual-sensor broadband seismic solutions.

The case studies conducted also emphasize the importance of careful processing and pre-conditioning especially of the pre-stack seismic data, and underscore the need to have these data as accurate as possible, particularly in terms of signal-to-noise ratio, amplitude linearity, flatness of the gathers, multiple suppression and preservation of frequency content across the offsets, etc.

Lithology fluid prediction

To further examine this aspect of increased reliability in the elastic attributes away from the well location, the next logical step is to assess more quantitatively the bandwidth extension benefits at the well location. This is illustrated by using cross-plots generated from a 2D example from the North West Shelf of Australia where pre-stack seismic inversion was performed on collocated conventional streamer and dual-sensor datasets. Both inversions were carried out using exactly the same parameters, with the same low frequency model and inversion parameters, with the exception of the wavelet estimation, which naturally had to be different, since there is significantly broader frequency content in the dual-sensor data compared to the conventional dataset. Therefore, the only difference between the two datasets is simply due to the type of streamer acquisition.

The dual-sensor seismic inversion results exhibit a clearer definition of the individual geological layers and the fluid contact. More importantly, the cross-plot analysis between the two is significantly different as illustrated in Figure 11. On this cross-plot of acoustic impedance versus Vp/Vs ratio the distribution of grey and red points extracted from the seismic inversion of the dual-sensor streamer data (Figure 11b) shows tighter clustering and a visually better match to the distribution of elastic properties extracted from the well which is not the case with the conventional seismic dataset shown in Figure 11a. This cross-plot comparison demonstrates clearly the better stability and lower noise in the pre-stack domain of the elastic reservoir properties, especially in the Vp/Vs-ratio using the dual-sensor streamer acquisition. In addition, the

slope of the tighter cluster is consistent with variations in porosity and hydrocarbon pore volume (HCPV).

The final case study from the Frigg Field (North Sea) reservoir of the North Viking Graben (see Figure 6) illustrates the estimation of lithology and fluid in 3D using the pre-stack seismic data comparing legacy/conventional and dual-sensor streamer datasets.

The Frigg gas field was discovered in 1971 and production was terminated after 27 years of production. It comprises a clastic reservoir of early Eocene age deposited in a deep marine environment and exhibits characteristic prograding submarine fan geometries on the seismic. The gas was discovered at a depth of around 2000 m and a clear flat-spot signature is evident on the seismic. Production ceased and decommissioning of the field started in 2004, however residual gas is still present which can be analyzed and mapped on this seismic dataset.

On these datasets a full quantitative interpretation has been performed including wavelet extraction, low frequency model generation, and pre-stack simultaneous inversion. Figure 12 illustrates the inversion results by comparing the acoustic impedance from the conventional and the recently acquired and processed dual-sensor seismic.

Before examining the lithology-facies classification itself, it is instructive to review the results of the acoustic impedance inversion between the conventional and the dual-sensor
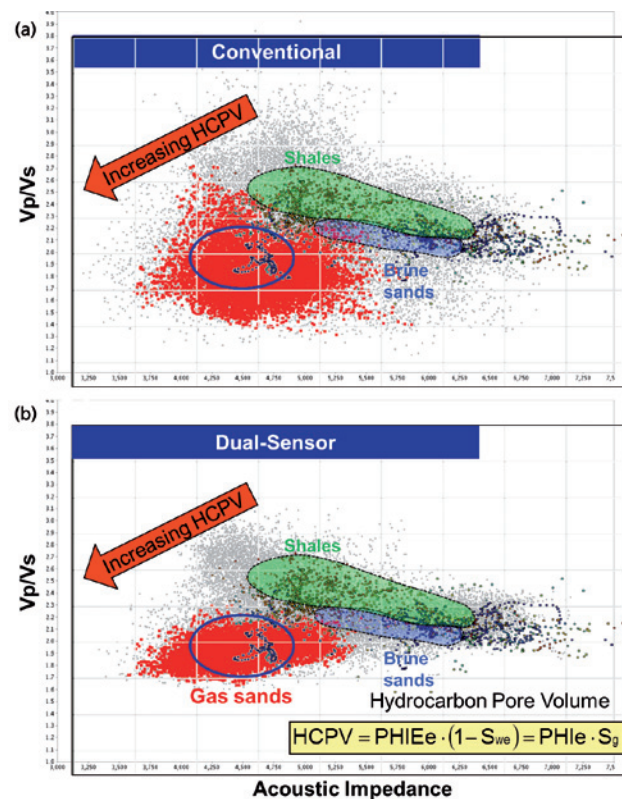

Figure 11 Cross-plot comparison between conventional (11a) and dual-sensor acquisition systems (11b) and well log information.
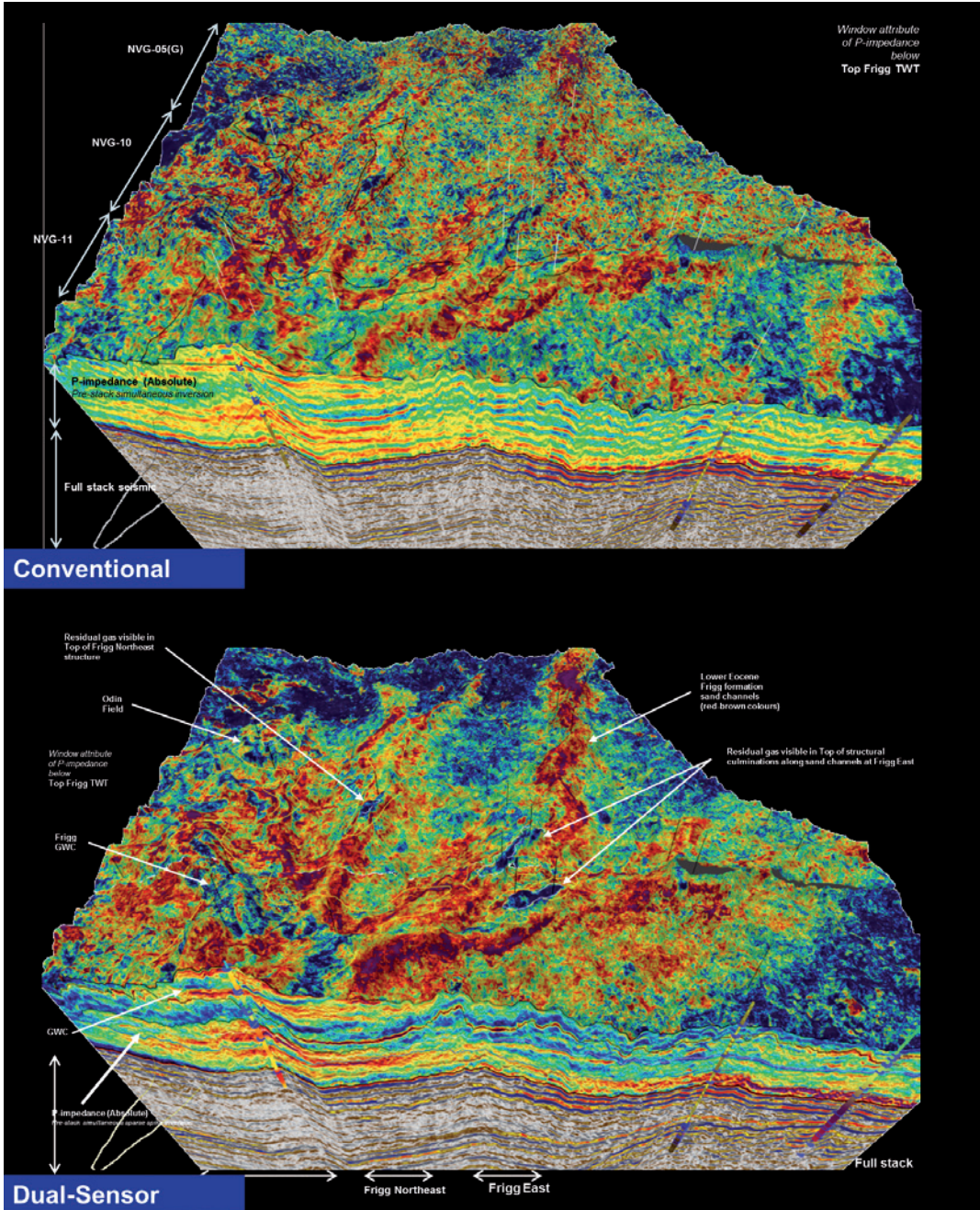
Reservoir Geoscience and Engineering

Figure 12 The top image represents the result of the acoustic impedance from the legacy dataset, the seismic inversion coming from the dual-sensor streamer is represented at the bottom.

seismic datasets illustrated in Figure 12. The main results of the comparison between the conventional and broadband seismic after pre-stack inversion are:

- Interpretability improvement by being able to delineate the various stratigraphic units, for instance the prograding foresets are better delineated on the broadband seismic data
- Better delineation of the main geological features by separating the sands and shale responses with the inversion results. As the dual-sensor seismic data are richer on the

low frequency side of the frequency spectrum, the side lobe imprint is significantly reduced improving the resolution of the inversion results, and providing a clearer discrimination of geological layers and less residual imprint of cyclical 'seismic' layering

- Significant improvement on the delineation of the channelized features: higher signal-to-noise ratio impedance with the broadband seismic, making the seismic impedance volume ideal for seismic structural and stratigraphic

Reservoir Geoscience and Engineering
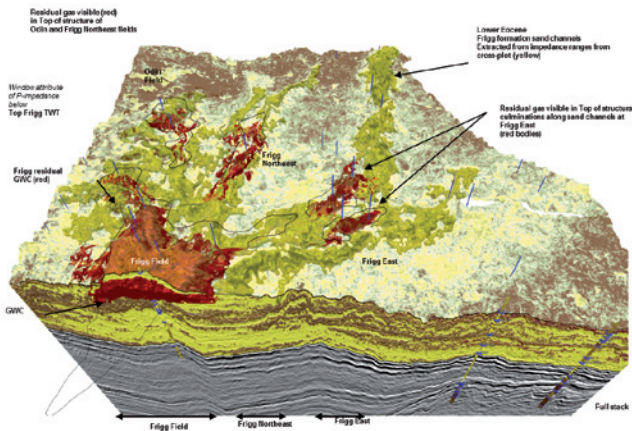
Figure 13 3D lithology fluid classification based on rock physics analysis. Results of the classification match the various field outlines like Frigg and Frigg East but also Odin (northwest of Frigg).

interpretation and the overall understanding of the geological depositional system.

The improvement in results from dual-sensor pre-stack analysis gave encouragement that a better understanding of the lithology and fluid distribution in this dataset could be achieved by lithology-fluid classification. Elastic attributes have been classified stochastically based on a rock physics analysis performed for the area. The lithology-fluid classification (Figure 13) highlights all the main geological features and field architecture and differentiates channel sands, hydrocarbon sands, and the shale layers forming the reservoir seal. By overlaying the various field outlines on the 3D lithology fluid classification, the residual gas in the Frigg, Frigg East, Odin, and various other hydrocarbon accumulations can be seen clearly, located on the structural culminations of discrete localized channel fairways.

Conclusion

The various examples presented here demonstrate that broadband seismic benefits not only the operations (increased weather acquisition window) and seismic processing aspects, but also the more 'downstream' part of the G&G cycle: interpretation and quantitative seismic interpretation.

The case studies shown demonstrate some of the benefits for the interpretation geoscientist in terms of the improved interpretability of broadband seismic as well as improved delineation of geological features. They also highlight that the extended seismic bandwidth of over an octave on both the low and high side reduces significantly the dependency on a priori information and improves the accuracy in the extracted elastic properties away from well control. The greater reliability of inversion results from dual-sensor seismic with less reliance on local well bias plays an important role in the evaluation and de-risking of prospects and leads as well as in well placement.

Broadband seismic without receiver and source ghosts opens the possibility of interpreting and analyzing the true earth response with significantly less filtering and interference effects.

Broadband seismic is therefore potentially beneficial across the asset life cycle from the beginning of the exploration stage to lithology and fluid prediction, optimized well placement, and resource estimation with constrained uncertainty in the appraisal and development stages.

References

Cambois, G., Osnes, B., Day, A. and Long, A. [2009] Dual Sensor Streamer Increases Data Bandwidth Leading to Improved Penetration and Higher Resolution. *EAGE Marine Seismic Workshop – Focus on Middle East & North Africa.*

Carlson, D., Long, A., Söllner, W., Tabti, H., Tenghamn, R. and Lunde, N. [2007] Increased resolution and penetration from a towed dual-sensor streamer. *First Break*, **25**(12), 71–77.

Engelmark, F and Reiser, C. [2010] Extending the low frequency content for improved processing, imaging, inversion and characterization. *SEG Low Frequency Workshop*, Snowbird, Utah.

Færseth, R.B. and Sætersmoen, B.H. [2008] Geometry of a major slump structure in the Storegga slide region offshore western Norway. *Norwegian Journal of Geology*, 88, 1–11.

Kelly, S., Ramos-Martinez, J. and Tsimelzon, B. [2009] The effect of improved, low-frequency bandwidth in full-waveform inversion for velocity. *79th SEG Annual International Meeting*, Expanded Abstract **28**, 3974–3978.

Ozdemir, H. [2009] Unbiased deterministic seismic inversion: more seismic, less model. *First Break*, **27**(11), 43–50.

Parkes, G. and Hegna, S. [2011] An acquisition system that extracts the earth response from seismic data. *First Break*, **29**(12), 81–87.

Parkes, G. and Hegna S. [2011] A marine seismic acquisition system that provides a full 'ghost-free' solution. *81st SEG Annual International Meeting*, Expanded Abstract, 37–41.

Reiser, C., Anderson, E. and Balabekov, Y. [2011] Improved Quantitative Interpretation with Broadband Seismic. *73rd EAGE Conference and Exhibition, Vienna*, Expanded Extract.

Reiser, C., Engelmark, F. and Anderson, E. [2012] Broadband seismic reviewed for the end-user benefits in interpretation and reservoir geophysics. *74th EAGE Conference and Exhibition*, Copenhagen.

Söllner et al. [2007] Surface-related multiple suppression in dual-sensor towed-streamer data. *77th SEG Annual Expanded Abstracts*.

Thompson, T., Lamont, M., Bevilacqua, C. and Hendrick, N. [2011] Fit for purpose seismic reservoir characterisation. *Petroleum Geology Conference and Exhibition*.

Whitcombe, D., Connolly, P., Reagan, R. and Redshaw, T. [2012] Extended Elastic Impedance for fluid and lithology prediction. *Geophysics*, **67**(1), 63–67.